

Crystallinity of Uniform Oligo(oxyethylene) Mono-alkyl Ethers studied by Raman Spectroscopy

John R. Craven,[†] K. Viras,[‡] Andrew J. Masters and Colin Booth*

Department of Chemistry, University of Manchester, Manchester M13 9PL, UK

Low-frequency Raman spectra have been recorded for two series of uniform oligo(oxyethylene) mono-*n*-alkyl ethers: α -alkyl, ω -hydroxyoligo(oxyethylene)s, $\text{H}(\text{CH}_2)_n(\text{OCH}_2\text{CH}_2)_m\text{OH}$, and α -alkyl, ω -methoxyoligo(oxyethylene)s, $\text{H}(\text{CH}_2)_n(\text{OCH}_2\text{CH}_2)_m\text{OCH}_3$. LAM-1 frequencies were identified and compared with those determined previously for *n*-alkanes, oligo(oxyethylene) di-*n*-alkyl ethers and oligo(oxyethylene) dimethyl ethers. On the basis of the linear crystal model of Minoni and Zerbi (*J. Phys. Chem.*, 1982, **86**, 4791), non-linear relationships between whole-chain LAM-1 frequency and reciprocal chain length have been explained as effects of end masses and end forces. Prominent bands in the spectra of the α -alkyl, ω -hydroxyoligo(oxyethylene)s were assigned to LAM-1 and LAM-3 of the H-bonded dimer crystallised in a bilayer structure.

We have recently reported on the solid-state structures of a number of specially synthesised poly(oxyethylene) *n*-alkyl ethers, investigated by small-angle X-ray and Raman scattering.¹ The materials used had distributions of oxyethylene chain lengths and, although the distributions were narrow ($M_w/M_n \leq 1.05$), the presence of oxyethylene blocks of different lengths was a complicating factor in the determination and interpretation of solid-state parameters, particularly for samples of short chain length which might fractionate during the crystallisation process.

Uniform oligomers are attractive model systems. The high-frequency Raman spectroscopy of uniform oligo(oxyethylene) mono-*n*-alkyl ethers in the solid state has been of interest in recent times. Matsuura, Fukuhara and co-workers (see, *e.g.* ref. 2-5) have paid attention to the molecular conformations of the alkyl (planar zig-zag) and oxyethylene (helical) blocks and have reported fully on the conformational transition in the oxyethylene block from extended to helical at chain lengths E_3 - E_4 , and also on details of the chain conformation at the oxyethylene/methylene boundary. Recently we have described⁶ a study of four series of uniform oligo(oxyethylene) mono-*n*-alkyl ethers by X-ray diffraction and differential scanning calorimetry. In this paper we report results obtained for the same samples by low-frequency Raman spectroscopy.

Two types of uniform oligo(oxyethylene) alkyl ether were prepared and investigated: α -alkyl, ω -hydroxyoligo(oxyethylene)s of general formula $\text{H}(\text{CH}_2)_n(\text{OCH}_2\text{CH}_2)_m\text{OH}$, denoted $C_nE_m\text{OH}$ to stress the presence of the terminal hydroxy group, and α -alkyl, ω -methoxyoligo(oxyethylene)s of general formula $\text{H}(\text{CH}_2)_n(\text{OCH}_2\text{CH}_2)_m\text{OCH}_3$, denoted $C_nE_mC_1$ to stress the similarity of the chain ends. In each case the oxyethylene chain lengths (m) were 4, 6, 8, 12 or 16 oxyethylene units and the alkyl chain lengths (n) were 9 or 15 methylene units. Oligomers $C_nE_6\text{OH}$ and $C_nE_6C_1$, with $n = 11$ or 13, were also studied. Overall chain lengths varied from 22 to 65 chain atoms, *i.e.* well below the critical length for chain folding in these materials.¹⁻⁷

We have already described⁸⁻¹² the low-frequency Raman spectra of uniform oligo(oxyethylene) di-*n*-alkyl ethers, $C_nE_mC_n$, which have solid-state structures in which the oxyethylene helices are orientated normal to the end-group plane

and close packed while the alkyl planar zig-zags are packed in a density-deficient layer,⁷⁻¹⁴ either liquid crystalline or crystalline depending on the alkyl block length. Raman scattering was observed from the very low frequency longitudinal vibration of the whole molecule and from the relatively high frequency longitudinal vibration of the alkyl blocks, the latter being effectively decoupled from the whole-molecule vibration. By reference to the results for oligo(oxyethylene)s,^{15,16} and with the aid of the perturbed elastic rod model of Hsu *et al.*,¹⁷ the whole-molecule vibrational mode was assigned to the longitudinal mode (LAM-1) of the low-modulus helical oxyethylene inner block perturbed by the alkyl blocks acting as inertial point masses at the ends of the chain and by end (interlayer) forces. The longitudinal mode of the high-modulus alkyl block was related in a straightforward way to the longitudinal mode (LAM-1) of an *n*-alkane of corresponding chain length.

The present work yields similar results for the uniform oligo(oxyethylene) monoalkyl ethers, but makes use of the more sophisticated linear chain model of Minoni and Zerbi.¹⁸

Experimental

Materials

The oligomers were prepared, purified and characterised as described earlier.¹⁹ Compositions of the oligomers were confirmed by mass spectrometry ($M < 700$, chemical ionisation in the presence of ammonia), ¹H NMR spectroscopy and elemental analysis. The nature of the end group, OH or OCH₃, was checked by IR spectroscopy, in which respect the oligomers were found to be >99% pure. The absence of oligomeric impurities was confirmed by GPC.

Raman Spectroscopy

Raman scattering at 90° to the incident beam was recorded by means of a Spex Ramalog spectrometer fitted with a 1403 double monochromator and a 1442U third monochromator and operated in scanning mode. The operation of the instrument was controlled by a DM1B Spectroscopy Laboratory Coordinator computer. The light source was a Coherent Innova 90 argon-ion laser operated at 514.5 nm and 400 mW. Operating conditions were chosen to suit the frequency range under investigation. Typical operating conditions were: high frequencies ($< 1800 \text{ cm}^{-1}$), bandwidth 5 cm^{-1} , scanning

[†] Present address: Domino-Amjet Ltd., Bar Hill, Cambridge CB3 8TU, UK.

[‡] Permanent address: National and Kapodistrian University of Athens, Department of Chemistry, Physical Chemistry Laboratory, Panepistimiopolis, 157 71 Athens, Greece.

increment 0.5 cm^{-1} , integration time 2 s; low frequencies ($<200\text{ cm}^{-1}$), bandwidth 1.5 cm^{-1} , scanning increment 0.1 cm^{-1} , integration time 3 s; very low frequencies ($<50\text{ cm}^{-1}$), bandwidth 1 cm^{-1} , scanning increment 0.05 cm^{-1} , integration time 4 s. The frequency scale was calibrated from time to time by reference to the spectrum of L-cystine and before recording each spectrum, to that of *n*-hexacosane. Generally a high-frequency spectrum was recorded immediately after a low-frequency spectrum, in order to confirm that the sample was unchanged by exposure to the laser beam. Fluorescence, if any, was minimised by leaving a sample in the laser beam for several hours before recording its spectrum.

Samples were enclosed in a capillary tube and held at a constant temperature ($\pm 1\text{ K}$) in the range 173–298 K by means of a Harney-Miller cell (available from Spex Industries Inc.). The intensity of a Raman band was observed over a period of time to ensure equilibration of the sample at a given temperature.

Results and Discussion

High-frequency Spectra

The high-frequency spectra (see Fig. 1) were unexceptional, displaying features anticipated^{2–5,20} for crystalline oligo(oxyethylene) alkyl ethers. The presence of bands characteristic of helical oxyethylene chains (the *ttg* sequence of bonds $\text{CH}_2\text{—O—CH}_2\text{—CH}_2$) at $500\text{--}600\text{ cm}^{-1}$ and $285\text{--}310\text{ cm}^{-1}$, and planar zig-zag alkyl chains (the all-*trans* conformation) at 1295 cm^{-1} and $1445\text{--}1466\text{ cm}^{-1}$, served to define the chain conformations of the component blocks.

Low-frequency Spectra

Spectra were recorded for each oligomer at several temperatures in the range from 173 K to the melting point: examples are shown later. Broad bands in the range $150\text{--}250\text{ cm}^{-1}$ (see Fig. 1 and Table 1) were assigned to the alkyl-block LAM-1, as discussed below. Bands at $75\text{--}90\text{ cm}^{-1}$, characteristic of oligo(oxyethylene)s at low temperatures,^{15,16,21} were also observed: as noted earlier, bands at *ca.* 80 cm^{-1} (optical mode) and 90 cm^{-1} (lattice mode) in the very low temperature spectra merged into a single broad peak when the sample temperature was raised. Other weak

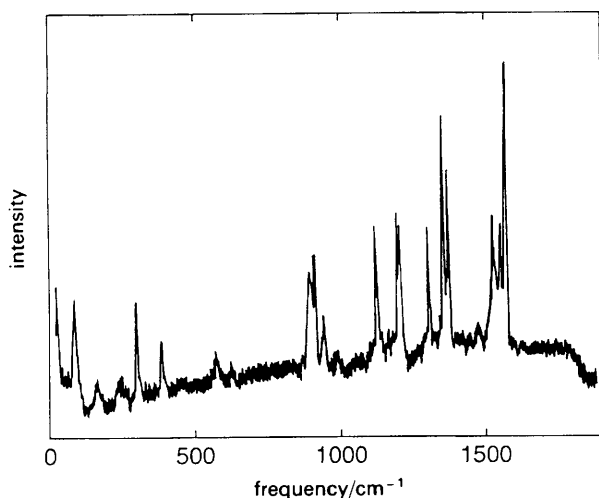


Fig. 1 Raman spectrum of α -pentadecyl- ω -hydroxydodecyl(oxyethylene), $\text{C}_{15}\text{E}_{12}\text{OH}$, at 173 K. The intensity scales and zeros are arbitrary

Table 1 Alkyl LAM-1 frequencies for uniform oligo(oxyethylene) monoalkyl ethers at 173 K

oligomers	frequency/ cm^{-1}
$\text{C}_{15}\text{E}_n\text{OH}/\text{C}_{15}\text{E}_n\text{C}_1$	153
$\text{C}_{13}\text{E}_6\text{OH}/\text{C}_{13}\text{E}_6\text{C}_1$	164
$\text{C}_{11}\text{E}_6\text{OH}/\text{C}_{11}\text{E}_6\text{C}_1$	204
$\text{C}_9\text{E}_n\text{OH}/\text{C}_9\text{E}_n\text{C}_1$	242

bands were observed, some of which have been previously identified in the spectra of oligo(oxyethylene)s.^{15,16,21,22} The positions of weak bands were confirmed by recording the spectra several times. A listing of verified band frequencies below 100 cm^{-1} is given in Tables 2 and 3: the assignment of the LAM-1 and LAM-3 bands is discussed below.

Alkyl-block LAM-1

The alkyl-block LAM-1 frequencies, listed in Table 1, depend on block length as illustrated in Fig. 2, where LAM-1 frequency is plotted against inverse alkyl block length ($1/n$). Comparison is made with the LAM-1 frequencies found previously for the alkyl blocks of oligo(oxyethylene) dialkyl ethers^{8–10} and for the *n*-alkanes of comparable chain length.²³ For both types of copolymer, the data points lie a little below the curve representing the results for the *n*-alkanes. This observation clearly supports the assignment to LAM-1 of the alkyl block and confirms their *trans*-planar

Table 2 Low-frequency Raman bands of uniform oligo(oxyethylene) monoalkyl ethers ($\text{C}_n\text{E}_m\text{C}_1$) at 173 K

oligomer	LAM-1 ^a / cm^{-1}	LAM-3 ^a / cm^{-1}	other bands/ cm^{-1}
$\text{C}_9\text{E}_{16}\text{C}_1$	21 (21)	41 (46)	85
$\text{C}_9\text{E}_{12}\text{C}_1$	24 (26)	— (58)	85
$\text{C}_9\text{E}_8\text{C}_1$	32 (33)	— (80)	16, 85
$\text{C}_9\text{E}_6\text{C}_1$	34 (38)	94 (102)	17, 56, 80
$\text{C}_9\text{E}_4\text{C}_1$	47 (48)	— (140)	9, 16, 29, 33, 57, 79
$\text{C}_{15}\text{E}_{16}\text{C}_1$	19 (20)	44 (44)	12, 30, 80, 87
$\text{C}_{15}\text{E}_{12}\text{C}_1$	22 (23)	57 (56)	7, 37, 82
$\text{C}_{15}\text{E}_8\text{C}_1$	28 (29)	— (79)	10, 21, 24, 42, 80, 83
$\text{C}_{15}\text{E}_6\text{C}_1$	— (35)	— (100)	19, 42, 84
$\text{C}_{15}\text{E}_4\text{C}_1$	46 (44)	138 (139)	7, 13, 19, 25, 30, 48, 56, 75

^a Calculated frequencies in parentheses: see text for details.

Table 3 Low-frequency Raman bands of uniform oligo(oxyethylene) monoalkyl ethers ($\text{C}_n\text{E}_m\text{OH}$) at 173 K

oligomer	LAM-1 ^a / cm^{-1}	LAM-3 ^a / cm^{-1}	other bands/ cm^{-1}
$\text{C}_9\text{E}_{16}\text{OH}$	11 (12)	24 (24)	30, 51, 86
$\text{C}_9\text{E}_{12}\text{OH}$	13 (15)	28 (29)	10, 20, 84
$\text{C}_9\text{E}_8\text{OH}$	17 (19)	32 (38)	7, 12, 29, 51, 80
$\text{C}_9\text{E}_6\text{OH}$	21 (22)	44 (46)	27, 82, 105
$\text{C}_9\text{E}_4\text{OH}$	26 (26)	60 (61)	37, 46, 81
$\text{C}_{15}\text{E}_{16}\text{OH}$	— (12)	— (22)	45, 80, 86
$\text{C}_{15}\text{E}_{12}\text{OH}$	12 (14)	26 (27)	9, 15, 21, 31, 40, 47, 60
$\text{C}_{15}\text{E}_8\text{OH}$	17 (17)	30 (35)	11, 19, 29
$\text{C}_{15}\text{E}_6\text{OH}$	18 (20)	44 (43)	28, 81
$\text{C}_{15}\text{E}_4\text{OH}$	21 (22)	56 (58)	7, 10, 40, 78

^a Calculated frequencies in parentheses: see text for details.

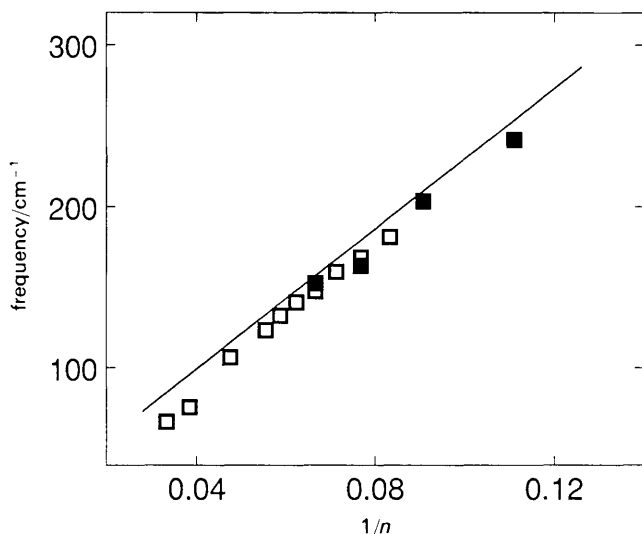


Fig. 2 Alkyl LAM-1 frequency vs. reciprocal alkyl chain length ($1/n$) for oligomers at 173 K: \blacksquare , oligo(oxyethylene) monoalkyl ethers, $C_nE_mC_1$ and C_nE_mOH ; \square , oligo(oxyethylene) di- n -alkyl ethers, $C_nE_mC_n$. The full line represents results for n -alkanes taken from ref. 23

conformation. The slightly lower LAM-1 frequency found for the oligomer, compared to the n -alkanes, reflects a damping effect of the low-modulus oxyethylene block.⁸

Oligomers $C_nE_mC_1$

Low-frequency spectra of oligomers $C_9E_mC_1$ are illustrated in Fig. 3: those of the C_{15} oligomers show similar features. In these spectra the predominant low-frequency band is that associated with the single-node longitudinal vibration of the whole molecule: this frequency is listed under LAM-1 in Table 2. The dependence of LAM-1 frequency on inverse oxyethylene block length [in chain atoms, $(3m+3)^{-1}$] is illustrated in Fig. 4. Comparison is made with the LAM-1 frequencies found²² for oligo(oxyethylene) dimethyl ethers of comparable chain length. The LAM-1 frequencies of the monoalkyl ethers deviate from those of the dimethyl ethers in a manner consistent with damping by the alkyl block acting as an inertial mass at one end of the chain. The generally lower frequencies found for the block oligomers with C_{15} blocks, compared to C_9 , reinforces this view.

In a previous study of poly(oxyethylene) alkyl ethers we used the perturbed elastic rod model of Hsu *et al.*¹⁷ to model the complex polydisperse oligomers. The corresponding approach for the present oligomers, which are of uniform composition and high crystallinity,⁶ is much simpler, and calculations made with sensible choices of parameters led to curves which fitted the results acceptably well. These calculations are not reproduced here, because we prefer to discuss the application of the linear chain model of Minoni and Zerbi,¹⁸ since this model can be readily adapted to deal with the more complicated case of the hydroxy-ended oligomers. A detailed comparison of the two approaches has been made earlier.²²

The Minoni-Zerbi model allows for the fact that the molecules are packed into layer crystals, and treats the case of the infinite one-dimensional crystal with an oligomeric repeat unit. If the alkyl block is treated as a point mass, as assumed earlier in treating dialkyl-ended oligomers,⁸ the required parameters are the force constants between chain groups (f_c) and between end groups (f_e) and the masses of chain groups (m_c) and end groups (m_e and m_a for methyl and alkyl,

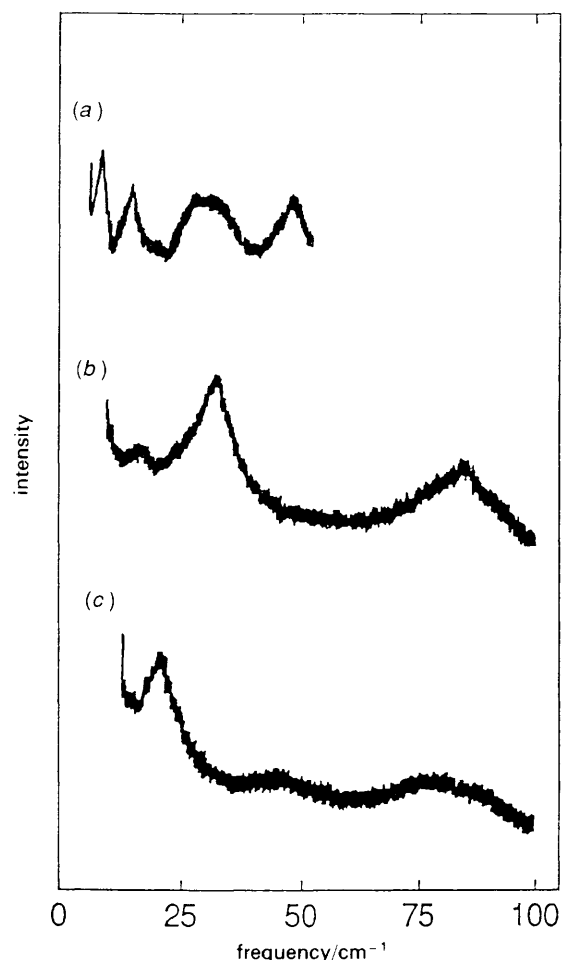


Fig. 3 Low-frequency Raman spectra of α -nonyl, ω -methoxy-oligo(oxyethylene)s at 173 K, (a) $C_9E_4C_1$, (b) $C_9E_8C_1$ and (c) $C_9E_{16}C_1$. The intensity scales and zeros are arbitrary

respectively), see Fig. 5. Note that the crystal structure illustrated in Fig. 5 is packed monolayers, as indicated by X-ray analysis.⁶ This unsymmetrical case was not treated by Minoni and Zerbi,¹⁸ but their equations are readily modified.

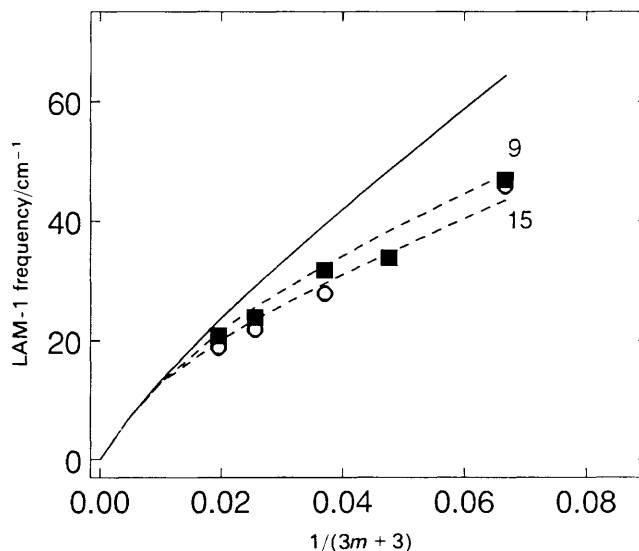


Fig. 4 LAM-1 frequency vs. reciprocal oxyethylene chain length [$1/(3m+3)$] for $C_nE_mC_1$ oligomers at 173 K: \blacksquare , $C_9E_mC_1$; \circ , $C_{15}E_mC_1$. The dashed curves are calculated, as described in the text, for the values of n indicated. The full curve represents the results for oligo(oxyethylene) dimethyl ethers, $C_1E_mC_1$, taken from ref. 22

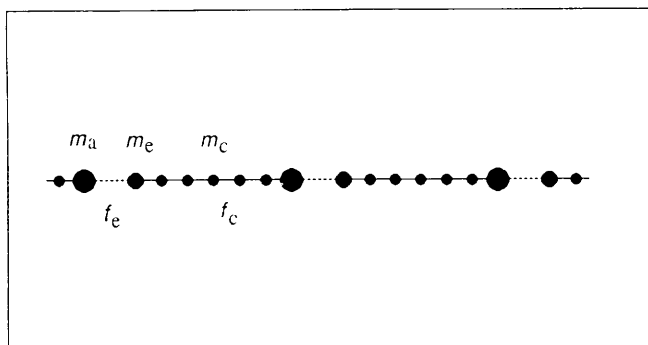


Fig. 5 Infinite one-dimensional crystal model for $C_n E_m C_1$ oligomers. Symbols m and f indicate masses and forces. Subscripts c, a and e indicate methylene chain units, alkyl end blocks and methyl end groups, respectively

The phase angle (θ) of the longitudinal vibration centred on the oligomer was calculated. For purposes of computation, the equations were used in the form:

$$X_{11} X_{22} - X_{12} X_{21} = 0$$

where

$$\begin{aligned} X_{11} &= 2f_c(m_e/m_c)(\cos \theta - 1)\sin \theta \\ &\quad - f_c\{\sin 2\theta - \sin \theta\} - f_e\{\sin x\theta - \sin \theta\} \\ X_{12} &= 2f_c(m_e/m_c)(\cos \theta - 1)\cos \theta \\ &\quad - f_c\{\cos 2\theta - \cos \theta\} - f_e\{\cos x\theta - \cos \theta\} \\ X_{21} &= 2f_c(m_a/m_c)(\cos \theta - 1)\sin x\theta \\ &\quad - f_c\{\sin(x-1)\theta - \sin x\theta\} - f_e\{\sin \theta - \sin x\theta\} \\ X_{22} &= 2f_c(m_a/m_c)(\cos \theta - 1)\cos x\theta \\ &\quad - f_c\{\cos(x-1)\theta - \cos x\theta\} - f_e\{\cos \theta - \cos x\theta\} \end{aligned}$$

and x is the chain length of the oxyethylene block in chain atoms (C and O), including both carbon atoms next to oxygen, *i.e.* $x = (3m + 3)$. The LAM frequency (ν) was obtained from:

$$(2\pi\nu)^2 = (2f_c/m_c)(1 - \cos \theta)$$

Calculations were carried out with the values of $f_c = 55 \text{ N m}^{-1}$ and $f_e = 2.5 \text{ N m}^{-1}$ used earlier^{22,24} for oligo(oxyethylene)s. The masses were $m_c = 2.439 \times 10^{-26} \text{ kg}$ (an average for the CH_2 and O groups), $m_e = 2.497 \times 10^{-26} \text{ kg}$ (CH_3) and $m_a = (2.329n + 0.167) \times 10^{-26} \text{ kg}$ (alkyl block).

The force constant used for the chain bonds ($f_c = 55 \text{ N m}^{-1}$) is equivalent to a longitudinal modulus for helical poly(oxyethylene) of $E = 2.5 \times 10^{10} \text{ N m}^{-2}$, as used earlier^{8,16,25} to fit results for methyl-ended and alkyl-ended oligo(oxyethylene)s. Song and Krimm^{26,27} have calculated LAM-1 frequencies for oligo(oxyethylene)s *via* normal-coordinate analysis and have shown that lateral interchain forces contribute to E . Here we assume that the effect of lateral forces can be subsumed into the composite chain force constant f_c .

The comparison of theory with experiment in Table 2 and Fig. 4 shows adequate agreement, particularly considering that we have used exactly the same parameters as previously.²² The general trends are well reproduced by the calculations. The difference in behaviour between the two systems (dimethyl and methyl alkyl ethers) is largest when the oxyethylene chain length is short, as expected since the effect on longitudinal vibrational frequency of a perturbing end mass will be greatest when a short chain is vibrating at relatively high frequency.

LAM-3 bands of the $C_n E_m C_1$ oligomers are weak and difficult to observe. Another problem is overlap with the strong optical and lattice bands at $75\text{--}90 \text{ cm}^{-1}$, which means that the LAM-3 bands of the shorter oligomers can be resolved. Guidance as to the position of LAM-3 cannot be obtained *via* the calculation, as indicated in Table 2.

Oligomers $C_n E_m \text{OH}$

Low-frequency spectra of oligomers $C_n E_m \text{OH}$ are illustrated in Fig. 6: those of the C_{15} oligomers show similar features. Generally there were two prominent low-frequency bands in the spectra, associated with the LAM-1 and LAM-3 longitudinal vibrations of the hydrogen-bonded dimer, as explained below: these frequencies are listed under LAM-1 and LAM-3 in Table 3.

The dependence of LAM-1 frequency on inverse oxyethylene block length [$1/(3m + 2)$] is illustrated in Fig. 7, where comparison is made with the LAM-1 frequencies calculated for the α -alkyl, ω -methoxy oligomers ($C_n E_m C_1$, see Fig. 4). The frequencies found for the $C_n E_m \text{OH}$ oligomers are about half those of the corresponding $C_n E_m C_1$ oligomers.

This marked effect is not explicable in terms of end forces, since a strong end force (hydrogen bond) should increase the frequency, nor can it be explained in terms of end masses, since the masses of the CH_3 and OH units are very similar. However, it is known⁶ that the hydroxy-ended oligomers crystallise into bilayers, by virtue of the formation of strong hydrogen bonds in the end-group plane. The present Raman

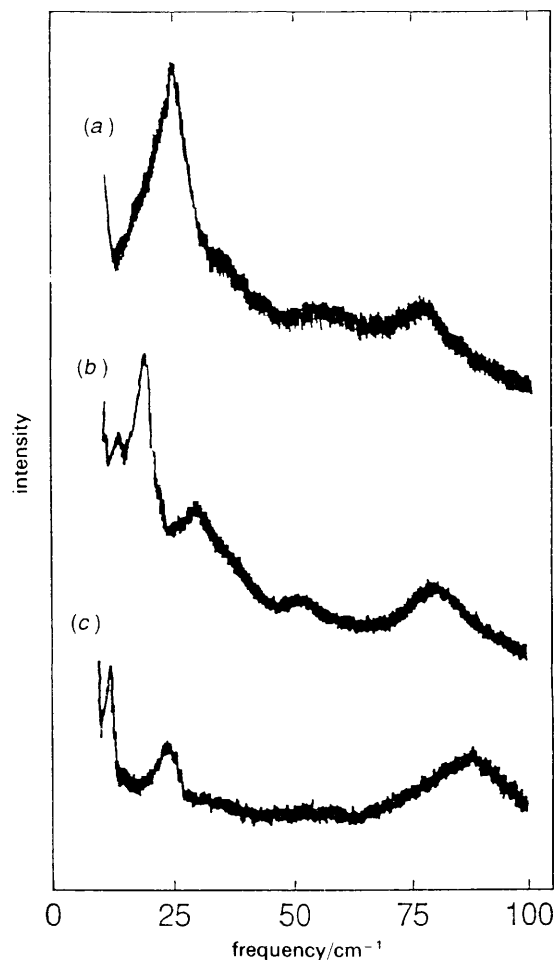


Fig. 6 Low-frequency Raman spectra of α -nonyl, ω -hydroxy-oligo(oxyethylene)s at 173 K: (a) $C_9 E_4 \text{OH}$, (b) $C_9 E_8 \text{OH}$ and (c) $C_9 E_{16} \text{OH}$ as indicated. The intensity scales and zeros are arbitrary

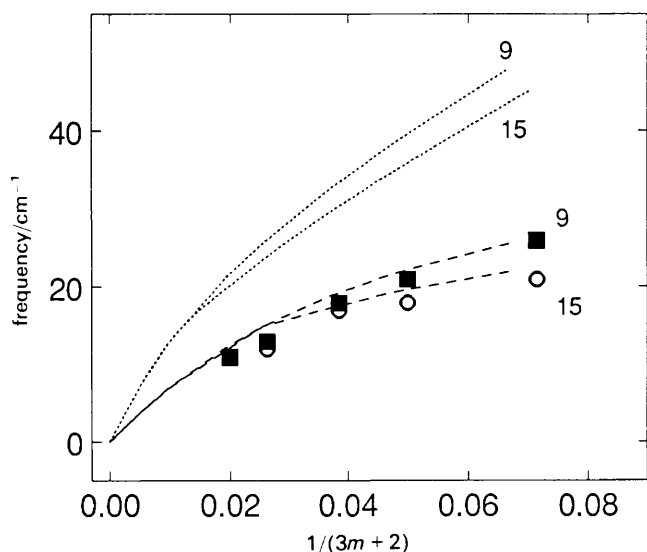


Fig. 7 LAM-1 frequency vs. reciprocal oxyethylene chain length [$1/(3m+2)$] for C_nE_mOH oligomers at 173 K: \blacksquare , C_9E_mOH ; \circ , $C_{15}E_mOH$. The dashed curves are calculated, as described in the text, for the values of n indicated. The dotted curves represent the results for $C_nE_mC_1$ oligomers ($m = 9$ and 15 as indicated) taken from Fig. 4

data are consistent with this view, with the further proviso that the hydrogen bonds link oligomers across the end-group plane, so as to couple the vibrations of two oligomers in the bilayer and thereby, effectively, double the length of the molecule so far as the LAM-1 frequency is concerned.

The one-dimensional crystal model of Minoni and Zerbi was used to confirm this conclusion. The vibrational frequencies of H-bonded dimers in a layer crystal in which they are subject to van der Waals end forces were calculated by use of the equations listed earlier²⁴ for the case of an infinite one-dimensional crystal with an H-bonded dimer repeat unit.^{23,28}

The notation used is indicated in Fig. 8. The methylene chain groups and the alkyl and hydroxy end groups are represented by point masses, m_c , m_a and m_h , respectively, and the interactions between them are represented by force constants f_c , f_e and f_h , respectively. The values used in applying the equations were those used above, plus additional values as used earlier,²⁴ $m_h = 2.8243 \times 10^{-26}$ kg, $f_h = 12$ N m⁻¹. Calculated frequencies are compared with observed frequencies in Table 3 and Fig. 7. Agreement is good, particularly considering that we have used exactly the same parameters as previously.²⁴

The frequencies calculated for the C_nE_mOH dimers are

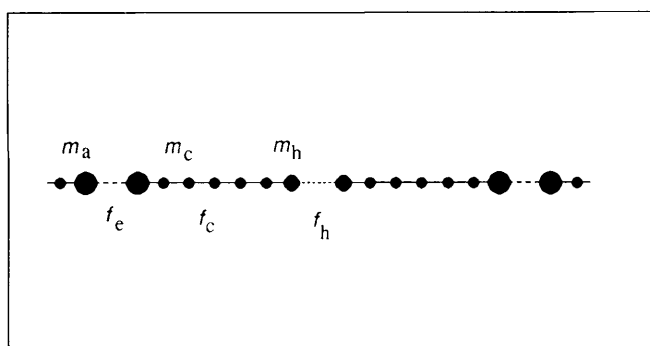


Fig. 8 Infinite one-dimensional crystal model for C_nE_mOH oligomers. Symbols m and f indicate masses and forces. Subscripts c , a and h indicate methylene chain units, alkyl end blocks and hydroxy end groups, respectively

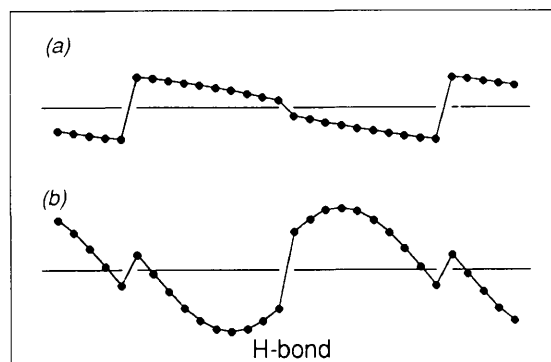


Fig. 9 Wave profiles for the H-bonded dimer: (a) LAM-1 (2 nodes per repeat unit of the infinite crystal) and (b) LAM-3 (4 nodes per repeat unit of the infinite crystal). The longitudinal displacements are represented as transverse

those for the first vibration in the series, *i.e.* the vibration with two nodes per dimeric repeat unit, as indicated in Fig. 9. As assumed above, this mode would normally be thought of as LAM-1 of the dimer. The next Raman-active vibrational mode has four nodes per repeat unit, see Fig. 9. This is LAM-3 of the dimer, which is equivalent to LAM-1 of the unimer if the node centred in the H-bond is discounted. This band is comparable in intensity with LAM-1 when the chain length is long, but is less readily observed in the spectra of the shorter oligomers.

Calculated LAM-3 frequencies are compared with observed values in Table 3. These dimer LAM-3 frequencies can also be compared with the LAM-1 frequencies calculated for the $C_9E_mC_1$ unimer (see Table 2). The higher frequencies calculated for LAM-3 of the dimer are consistent with a stronger (hydrogen-bonded) end force.

Temperature Dependence of LAM-1

Spectra recorded over a temperature range showed that the LAM-1 frequencies decreased as temperature increased at a rate of *ca.* -2 cm⁻¹ per 100 K. This temperature dependence is very similar to that found for other uniform oligomers; *e.g.* n -alkanes²³ and oligo(oxyethylene) di-methyl ethers.²²

Point Masses

The assumption that the alkyl block can be represented as a point mass is an obvious oversimplification. A detailed study⁸ of uniform dialkyl pentadecyl(oxyethylene)s, $C_nE_{15}C_n$, revealed a transition in the chain length dependence of LAM-1 frequency: *i.e.* the LAM-1 frequency was found to be constant over the range of alkyl chain lengths C_8 – C_{13} . This was not explicable in terms of a simple model (in that case the rod model) and the effect was associated⁸ with a change in structure from partly crystalline (type I) to wholly crystalline (type II) oligomers as the alkyl block length was increased at constant oxyethylene block length, and attributed to an effect of intermolecular interactions in the n -alkane region of the layer crystal. Such interactions could affect both the overall chain force constant f_c and the end force constant f_e .

There are irregularities in the present data (see Fig. 4 and 7) which are not explained in the discussion above. DSC measurements of enthalpy of fusion⁶ also show significant irregularities. A contributory factor may be that the oligomers form solid-state structures which fall between type I (*i.e.* crystalline oxyethylene blocks, liquid crystalline alkyl blocks) and type II (*i.e.* completely crystalline). However, the point

cannot be pursued, as the present results relate mainly to changing the oxyethylene block length rather than the alkyl block length.

Prof. D.L. Dorset kindly provided a number of samples related to those described in this paper. Drs. D. Jackson and E.J. Goodwin (ICI Chemicals and Polymers) took an interest in the work. Messrs. P. Kobryn and K. Nixon assisted with the experimental measurements. The British Council and the Royal Society gave financial support.

References

- 1 K. Viras, F. Viras, C. Campbell, T. A. King and C. Booth, *J. Chem. Soc., Faraday Trans. 2*, 1987, **83**, 917.
- 2 H. Matsuura and K. Fukuhara, *J. Phys. Chem.*, 1986, **90**, 3057.
- 3 H. Matsuura and K. Fukuhara, *J. Phys. Chem.*, 1987, **91**, 6139.
- 4 H. Matsuura and K. Fukuhara, *J. Mol. Struct.*, 1988, **189**, 249.
- 5 H. Matsuura, K. Fukuhara, S. Masatoki and M. Sakakibara, *J. Am. Chem. Soc.*, 1991, **113**, 1193.
- 6 J. R. Craven, H. Zhang and C. Booth, *J. Chem. Soc., Faraday Trans.*, 1991, **87**, 1183.
- 7 S. G. Yeates and C. Booth, *Makromol. Chem.*, 1985, **186**, 2663.
- 8 T. G. E. Swales, H. H. Teo, R. C. Domszy, K. Viras, T. A. King and C. Booth, *J. Polym. Sci., Polym. Phys. Ed.*, 1983, **21**, 1501.
- 9 S. G. Yeates, H. H. Teo and C. Booth, *Makromol. Chem.*, 1984, **185**, 2475.
- 10 S. G. Yeates and C. Booth, *Eur. Polym. J.*, 1985, **21**, 217.
- 11 K. Viras, T. A. King and C. Booth, *J. Chem. Soc., Faraday Trans. 2*, 1985, **81**, 491.
- 12 K. Viras, T. A. King and C. Booth, *J. Chem. Soc., Faraday Trans. 2*, 1985, **81**, 1477.
- 13 R. C. Domszy and C. Booth, *Makromol. Chem.*, 1982, **183**, 1051.
- 14 H. H. Teo, T. G. E. Swales, R. C. Domszy, F. Heatley and C. Booth, *Makromol. Chem.*, 1983, **184**, 861.
- 15 K. Viras, H. H. Teo, A. Marshall, T. A. King and C. Booth, *J. Polym. Sci., Polym. Phys. Ed.*, 1983, **21**, 919.
- 16 K. Viras, T. A. King and C. Booth, *J. Polym. Sci., Polym. Phys. Ed.*, 1985, **23**, 471.
- 17 S. L. Hsu, G. W. Ford and S. J. Krimm, *J. Polym. Sci., Polym. Phys. Ed.*, 1977, **15**, 1769.
- 18 G. Minoni and G. Zerbi, *J. Phys. Chem.*, 1982, **86**, 4791.
- 19 J. R. Craven, R. H. Mobbs, C. Booth, E. J. Goodwin and D. Jackson, *Makromol. Chem.*, 1989, **190**, 1207.
- 20 J. L. Koenig and A. C. Angood, *J. Polym. Sci., Part A-2*, 1970, **8**, 1787.
- 21 J. F. Rabolt, K. W. Johnson and R. W. Zitter, *J. Chem. Phys.*, 1974, **61**, 504.
- 22 C. Campbell, K. Viras and C. Booth, *J. Polym. Sci., Polym. Phys. Ed.*, in the press.
- 23 H. G. Olf and B. Fanconi, *J. Chem. Phys.*, 1973, **59**, 534.
- 24 C. Campbell, K. Viras, A. J. Masters, J. R. Craven, H. Zhang, S. G. Yeates and C. Booth, *J. Phys. Chem.*, 1991, **87**, 4647.
- 25 F. Viras, K. Viras, C. Campbell, T. A. King and C. Booth, *J. Chem. Soc., Faraday Trans. 2*, 1987, **83**, 927.
- 26 K. Song and S. Krimm, *Macromolecules*, 1989, **22**, 1504.
- 27 K. Song and S. Krimm, *J. Polym. Sci., Polym. Phys. Ed.*, 1990, **28**, 35; 51; 63.
- 28 G. Minoni, G. Zerbi and J. F. Rabolt, *J. Chem. Phys.*, 1984, **81**, 4782.

Paper 1/03408A; Received 8th July, 1991